Exploring new molecular imaging concepts of prostate cancer

Wondergem, Maurits

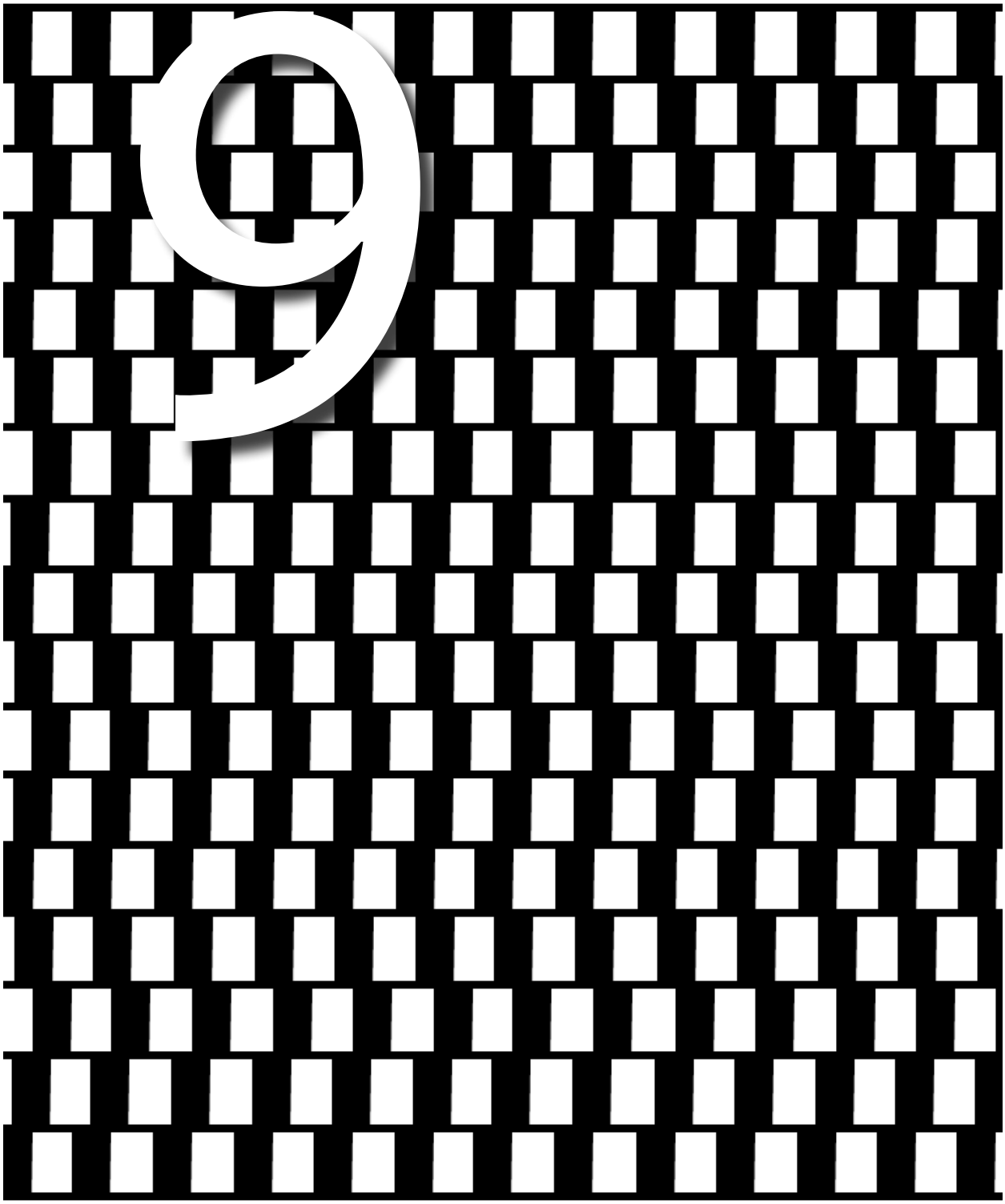

Summary

Chapter 1 comprises a general introduction of the topic of this thesis as well as its aim and outline. In the general introduction the extent of prostate cancer as a health care problem is pictured by epidemiological aspects and by discussion of the heterogeneous character of the disease, which makes it challenging to apply the optimal treatment to the right patient at the right moment. The TNM- staging system is introduced and tools available for clinicians to stage the disease and choose the optimal treatment are discussed *(1)*. Amongst other tools, imaging techniques play a pivotal role at different stages of the disease. Nuclear Imaging techniques are used particularly for detection of metastases of which lymph node and bone metastases are most frequent. Those techniques include planar scintigraphy, Single Photon Emission Computed Tomography (SPECT), Positron Emission Tomography (PET) and hybrid techniques, which synergise the information of biological activity from SPECT or PET with anatomical information from commonly Computed Tomography (CT) *(2-7)*.

Depending on the course of the disease and the estimated risk on lymph node or bone metastases, different tracers and techniques are used in Nuclear Medicine. Some of them only show the secondary process of bone remodelling due to metastatic infiltration in the bone matrix, while others show the localisation of tumour cells themselves and could therefore also be used to image the primary tumour and soft tissue metastases. Tracers that image bone remodelling include ^{99m}Tc-MDP and ^{99m}Tc-HDP, and have been used for decades *(8)*. However, there is renewed interest in ^{18}F-sodiumfluoride (NaF), which was already used as a bone tracer before ^{99m}Tc-diphosphonates became available *(9)*. The last decades a diversity of molecules have been synthesised that may serve as tracers of tumour cells. Some of them showed potential for imaging of prostate cancer cells and a selection of these potential tracers together with the pathways they visualise are shortly discussed. Choline based tracers and tracers that target Prostate Specific Membrane Antigen (PSMA) are becoming integrated in standard clinical practice and are discussed in more depth *(10-12)*. Aspects including history and pre-clinical research, pharmacokinetics, cellular uptake, and biodistribution including physiological and pathological uptake, are discussed for the tracers studied in this thesis: ^{99m}Tc-MDP, ^{99m}Tc-HDP, NaF, ^{11}C-choline, ^{18}F-fluorocholine and ^{18}F-DCFPyL. Once available for use in patients, insights in clinical aspects including diagnostic accuracy, optimal patient preparation and optimal acquisition parameters are needed before tracers can be incorporated in standard clinical care.

For BS wide ranges in sensitivity and specificity, from less than 50% up to 100%, are reported in literature. In general it is stated that BS has a reasonable sensitivity with a low specificity *(6, 13)*. In ***chapter 2*** the diagnostic accuracy of NaF PET(/CT), ^{11}C-choline PET(/CT) and ^{18}F-fluorochline PET/(CT) is studied by means of a systematic literature review. The rationale for superior diagnostic performance of those techniques may be found in the use of PET instead of planar scintigraphy or SPECT, which results in enhanced image quality, and also in the favourable biological kinetics of especially NaF over ^{99m}Tc-HDP. NaF has a three times better target-to-background ratio than ^{99m}Tc-

diphosphonates *(14)*. Choline-based tracers directly target tumour cells and may detect bone metastases that have not yet affected the surrounding bone tissue.

A comprehensive literature search was performed using the Medline database. Thirteen studies were eligible for inclusion in the review. All studies are summarised in the review. Data from the included studies was pooled. On a lesion basis a pooled-weighted sensitivity and specificity of respectively 84 and 98% was found for PET/CT with choline-based tracers and 89 and 91% for NaF PET/CT. On a patient basis performances of 85 and 97% for choline-based tracers and 87 and 80% for NaF were found. In conclusion the literature provided evidence for better detection of bone metastases of both NaF and choline-based tracers compared to conventional BS.

Included studies in the review were heterogeneous in many aspects and included relatively small cohorts and therefore in ***chapter 3*** the diagnostic performance of BS and NaF PET/CT is studied in two large retrospective cohorts of patients that were initially staged for high-risk prostate cancer. A composite reference standard (RS) was used, which comprised a follow-up of at least 18 months for the BS cohort and at least 6 months for the NaF PET/CT cohort, and included staging imaging, follow-up imaging (BS, Magnetic Resonance Imaging (MRI), CT, X-ray, ^{18}F-fluorocholine PET/CT, and/or ^{18}F-FDG PET/CT), biochemical follow-up and clinical follow-up. The diagnostic performances of each modality were calculated by comparison of the BS and NaF PET/CT results with the RS.

The BS cohort and NaF PET/CT cohort included 122 and 104 analysed patients, respectively. With BS and NaF-PET/CT respectively, lesions characteristic for bone metastases were found in 27 and 59%, no signs of metastases in 50 and 39% and equivocal results in 23 and 3%. In order to account for equivocal findings, the diagnostic characteristics were calculated under the assumption that equivocal BSs and NaF PET/CTs were positive and calculated again assuming that the equivocal scans were negative. Calculated sensitivities ranged from 84 to 95% and from 97 to 100% for BS and NaF PET/CT, respectively, and specificities ranged from 72 to 100% and 98 to 100%. Overall accuracy of BS ranged from 79 to 95% and for NaF PET/CT from 98 to 99%. The observed favourable diagnostic characteristics of NaF PET/CT compared to BS are in line with currently available literature, which is also reviewed in chapter 2.

Equivocal findings resulted in additional imaging procedures in 16% of all patients in the BS cohort and 2% in the NaF PET/CT cohort. In addition to bone metastases NaF PET/CT may diagnose lymph node metastases and these were found on low-dose CT in 50% of the patients in the NaF cohort, of which 13 patients had no signs of bone metastases.

Due to the nature of the study, differences between both cohorts in terms of patient characteristics were observed. To overcome this problem the cohorts were subcategorised by PSA value and Gleason-score. In most PSA categories and all Gleason-score categories NaF PET/CT detected bone metastases in a higher percentage of patients.

In ***chapter 4*** the scope is focused at ^{18}F-fluorocholine PET/CT. Variability is found in reported sensitivity and specificity for detection of prostate cancer metastases with ^{18}F-fluorocholine PET/CT, which may be due to lack of standardisation of imaging protocols *(15)*. Studies with relatively small patient populations showed different ^{18}F-fluorocholine activity patterns over time for both non-malignant and malignant tissues and lesions. Based on this variety of patterns different recommendations are given regarding the time point of image acquisition, including single, dual and triple time point protocols *(16-18)*. Therefore kinetics of ^{18}F-fluorocholine were studied in malignant lesions (lymph node metastases and bone metastases) and non-malignant tissues that might interfere with detection of those metastases.

One hundred subsequent patients that received ^{18}F-fluorocholine PET/CT for detection of prostate cancer lesions were prospectively included in the study. A dynamic acquisition of the pelvis was started immediately after administration of the tracer, which lasted for 10 minutes. Late static total body images were acquired 45 to 60 minutes after administration. Time activity curves (TAC) were constructed for lymph node metastases, bone metastases, non-malignant lymph nodes, non-malignant bone, adipose tissue, muscle, intestine and blood pool. ^{18}F-fluorocholine uptake by means of the maximal Standardised Uptake Value (SUV_{max}) between early and late acquisition time points was analysed and compared.

The TACs showed rapid ^{18}F-fluorocholine uptake in both malignant lesions and non-malignant tissues resulting in nearly constant concentrations 2 minutes after injection. However, for non-malignant lymph nodes a statistically significant decreasing SUV_{max} over time was found while muscle, malignant bone lesions and non-malignant bone showed increasing SUV_{max} over time. As expected blood pool activity decreased over time.

Two bone lesions (9%) were seen on early images only. This may be explained by more progressive ^{18}F-fluorocholine uptake in muscle tissue than in malignant lesions over time. Another explanation of this phenomenon could be imaging of blood flow in the tumour at early time point without tracer deposition resulting in absent activity at the late time point.

A RS consisting of a follow-up period of at least 9 months was used to determine whether target lesions were malignant or benign. ROC analysis was performed in order to find best predictors for malignancy in lymph node and bone lesions. The true nature of 6 malignant lymph nodes and 2 malignant bone lesions could not be established by the RS, while all non-malignant lymph nodes and bone lesions proved to be benign. As a result ROC analyses were performed with the assumption that all suspected lesions were malignant and with the assumption that all unconfirmed lesions were benign. For lymph nodes $SUV_{max,late}$ was found to be the best predictor of malignancy with a cut-off value between 1.9 and 2.0. For bone lesions $SUV_{max,early}$ and $SUV_{max,late}$ were both found to be best predictors of malignancy with a cut-off value of 2.5 and 2.9 respectively, irrespective of the chosen assumption.

The uptake pattern of ^{18}F-fluorocholine may also help to discriminate malignant from benign lymph nodes. Increasing ^{18}F-fluorocholine over time is highly specific (100%) for malignancy, with a modest sensitivity of 62%.

It was concluded that combined image acquisition at both an early and late time point has advantages over a single late time point acquisition. Given the better ability to discriminate malignant and non-malignant lymph nodes at late images, while addition of early images helped to further discriminate lymph nodes and improved detection of bone lesions.

Detection of lymph node metastases may be hampered by high physiological choline uptake in the gastrointestinal tract commonly seen on ^{11}C-choline or ^{18}F-fluorocholine PET/CT. In literature, fasting is frequently advised before ^{18}F-fluorocholine PET/CT and four hours of fasting before administration of ^{11}C-choline is suggested in a document of the Society of Nuclear Medicine and Molecular Imaging *(19, 20)*. There is no evidence that supports fasting prior to choline ^{11}C-choline or ^{18}F-flurocholine PET/CT. In ***chapter 5*** the impact of fasting for at least 6 hours, on the ^{18}F-fluorocholine uptake in the gastrointestinal tract is studied. Two cohorts of 40 patients scanned with ^{18}F-fluorocholine PET/CT were studied. The first cohort consisted of patients that did not fast before ^{18}F-flurocholine PET/CT, while patients in the second cohort fasted for at least 6 hours prior to PET/CT.

Dynamic data showed a similar uptake pattern for both cohorts in the intestines in the first 10 minutes after administration and no statistical differences were found at any time point. Late data acquired approximately 45 minutes after tracer injection were used to determine the ^{18}F-fluorocholine uptake in liver, spleen, stomach, pancreas and intestine. Intestinal uptake was measured in five different regions: 1 cm or less in the proximity of the aorta, both left and right common iliac arteries and both left and right external iliac arteries. In all studied regions, no differences were found in ^{18}F-fluorcholine uptake (SUV_{max} and SUV_{peak}) between both cohorts. In all patients high ^{18}F-fluorocholine activity, which might interfere with detection of lymph node metastases, was found near the aorta. In both cohorts, over half of the patients showed activity near the left and right external iliac artery and right common artery, while in almost half of the patients activity was found near the left common iliac artery.

Intensity of intestinal activity was found to be comparable with activity in malignant lymph nodes, with a SUV_{max} of approximately 4 for both groups. Therefore, interference of physiological activity in the intestine with detection of lymph node metastases was shown to be realistic. However it was concluded that fasting had no impact on uptake in the gastrointestinal tract and should not be recommended before ^{18}F-fluorocholine PET/CT.

^{11}C-choline and ^{18}F-fluorocholine are typically used for detection of metastases. However, there is literature showing that those tracers are able to diagnose local relapse after

radical prostatectomy. Timing of image acquisition may significantly influence the detection rate and significantly increased detection of local prostate cancer recurrence is seen with an acquisition protocol including an early dynamic study of the pelvis starting immediately after intravenous injection of ^{18}F-fluorocholine. In patients with PSA ≤1.0 ng/ml a detection rate of 76% was found (111/146 patients). Of those 111 scans 99 showed ^{18}F-fluorocholine uptake in the surgical bed only, which was interpreted as local recurrence. In 80/99 patients (84%), ^{18}F-fluorocholine uptake was seen on early dynamic images only.

In our daily clinical practice we did not notice such high detection rates of local recurrence with ^{18}F-fluorocholine PET/CT in patients with biochemical recurrence after radical prostatectomy, despite standard image acquisition of the pelvis immediately after injection of ^{18}F-fluorocholine. Incorrect interpretation of focal ^{18}F-fluorocholine uptake in the prostate bed, seen on early images only, may have major consequences for clinical management. Especially in patients that already received salvage radiation therapy after radical prostatectomy, renewed signs of local recurrence will prohibit any treatment with curative intent.

Therefore, in ***chapter 6*** the occurrence rate of focally increased ^{18}F-fluorocholine uptake in and near the prostatic fossa on both early and late images was evaluated in a cohort of patients scanned with ^{18}F-fluorocholine PET/CT with a biochemical relapse after radical prostatectomy. Additionally a second cohort, which included patients that received ^{18}F-fluorocholine PET/CT for primary staging, was studied to determine whether increased tracer uptake on early images is also present in a totally different patient population and to determine whether this represents prostate cancer lesions.

Forty patients with a biochemical relapse and 25 patients with primary prostate cancer were analysed. On early images only, focally increased ^{18}F-fluorocholine uptake in the prostatic bed region was seen in 28/40 patients (70%) and in 11/25 patients (44%) after prostatectomy and at initial staging, respectively. Fusion of PET and CT images revealed that all those lesions were located in the penile bulb. For patients after radical prostatectomy it could be postulated that these focal activities are a sign of local recurrence at the vesicoureteral anastomosis. However, for patients at initial staging it is highly unlikely that those findings represent prostate cancer depositions located in the penile bulb.

Furthermore, the time-activity patterns of those lesions in the penile bulb showed a similar course in both cohorts suggesting that those observations represent the same substrate. Blood pool activity showed a similar pattern as compared to the pattern found for the focal activities in the penile bulb. Since the penile bulb is a highly perfused structure, physiological ^{18}F-fluorocholine uptake in this structure is expected to follow the uptake pattern of the blood pool.

Furthermore, in patients scanned at initial staging, the time activity patterns of the biopsy confirmed primary prostate tumour, of lymph nodes suspicious of metastases, and of malignant bone lesions all showed the same pattern, which was clearly different from the pattern observed in the penile bulb. This is another indication that focal activity in the penile bulb after radical prostatectomy does not represent local relapse of prostate cancer.

It was concluded that focally increased ^{18}F-fluorocholine activity in the prostatic region seen on early images only is found in a high number of patients referred for evaluation after biochemical relapse and those referred for primary staging and, according to our data, represents physiological uptake in the penile bulb. Accurate discrimination of this phenomenon is important since incorrect interpretation may have major consequences for clinical management.

In comparison with Choline PET/CT, PSMA-tracers have shown to detect more lesions at lower PSA levels, which increases the sensitivity for prostate cancer and increases the clinical impact of PET/CT in prostate cancer *(12, 21)*. Furthermore, the specific binding to PSMA increases specificity for prostate cancer and positive predicting values. Literature on PSMA-tracer kinetics show that the tracer accumulates in prostate cancer cells over time while background activity decreases *(22-26)*. For ^{68}Ga-PSMA tracers it has been reported that late imaging at 180 min post injection (p.i.) instead of imaging at 45-60 min p.i improves detection of prostate cancer lesions *(27)*. In a recent pilot study ^{18}F-DCFPyL demonstrated higher tumour radiotracer uptake and higher tumour-to-background ratios in 9 patients on images acquired 120 min p.i. as compared to images obtained at 60 min p.i. *(28)*. In order to build upon these findings of improved lesion detection at later time-points, the effects of PET/CT imaging at 120 minutes p.i. of ^{18}F-DCFPyL in comparison to images acquired 60 minutes p.i. in a clinical cohort of patients with histopathologically proven prostate cancer is studied in ***chapter 7***.

By visual analysis, in 25/65 patients (38,5%) images at 120 min p.i. showed more lesions with enhanced ^{18}F-DCFPyL uptake as compared to the images acquired at 60 min p.i. and all lesions visible on 60 min p.i. images were also visible at 120 min p.i.. According to the presently used TNM classification (seventh edition) 6 patients (9.2%) had a higher disease stage on 120 min p.i images compared to images acquired at 60 min p.i.. One patient was up-staged from N0M0 to N1M1a, 2 patients from N0M0 to N1M0, 2 patients from N1M0 to N1M1a and 1 patient from N0M0 to N0M1b.

Thirty prostate lesions, 6 seminal vesicle lesions, 125 lymph nodes (81 local and 44 distant lymph nodes) and 42 skeletal lesions were included in a quantitative analysis. Overall a statistically significant increase in ^{18}F-DCFPyL uptake over time was seen in the 203 lesions characteristic for prostate cancer. Median SUV_{max} increased from 10.8 to 12.9 ($p<0.001$, Wilcoxon singed rank test). Also for all individual anatomical regions, including prostate, seminal vesicles, local lymph nodes, distant lymph nodes and skeletal lesions an overall significant increase in ^{18}F-DCFPyl uptake over time was found.

According to image quality as measured by the SNR in the liver in all 65 included patients, a variable course over time on a per patient basis was found. However by statistical analysis a significant better mean $SNR_{120\ min\ p.i.}$ of 11.93 was found ($p<0.001$, paired T-test, $SNR_{60\ min\ p.i.}$ 11.15).

It was concluded that imaging 120 min p.i. is superior to imaging 60 min p.i. with respect to lesion detection without deterioration of image quality. Further studies are needed to elucidate the best imaging time point for ^{18}F-DCFPyL.

REFERENCES

1. National Comprehensive Cancer Network. NCCN Clinical Practice Guidelines in Oncology: Prostate Cancer V. 1. 2015. Available at http://www.nccn.org/professionals/physician_gls/pdf/prostate.pdf. Accessed: May 4, 2017.
2. Abuzallouf S, Dayes I, Lukka H. Baseline staging of newly diagnosed prostate cancer: A summary of the literature. *J Urol*. 2004;171:2122-2127.
3. Dickinson L, Ahmed HU, Allen C, et al. Magnetic resonance imaging for the detection, localisation, and characterisation of prostate cancer: Recommendations from a european consensus meeting. *Eur Urol*. 2011;59:477-494.
4. Rorvik J, Halvorsen OJ, Albrektsen G, Haukaas S. Lymphangiography combined with biopsy and computer tomography to detect lymph node metastases in localized prostate cancer. *Scand J Urol Nephrol*. 1998;32:116-119.
5. Van Poppel H, Ameye F, Oyen R, Van de Voorde W, Baert L. Accuracy of combined computerized tomography and fine needle aspiration cytology in lymph node staging of localized prostatic carcinoma. *J Urol*. 1994;151:1310-1314.
6. Even-Sapir E, Metser U, Mishani E, Lievshitz G, Lerman H, Leibovitch I. The detection of bone metastases in patients with high-risk prostate cancer: 99mTc-MDP planar bone scintigraphy, single- and multi-field-of-view SPECT, 18F-fluoride PET, and 18F-fluoride PET/CT. *J Nucl Med*. 2006;47:287-297.
7. Herlemann A, Wenter V, Kretschmer A, et al. 68Ga-PSMA positron emission tomography/computed tomography provides accurate staging of lymph node regions prior to lymph node dissection in patients with prostate cancer. *Eur Urol*. 2016;70:553-557.
8. Van den Wyngaert T, Strobel K, Kampen WU, et al. The EANM practice guidelines for bone scintigraphy. *Eur J Nucl Med Mol Imaging*. 2016;43:1723-1738.
9. Blau M, Nagler W, Bender MA. Fluorine-18: A new isotope for bone scanning. *J Nucl Med*. 1962;3:332-334.
10. Hara T, Kosaka N, Kishi H. PET imaging of prostate cancer using carbon-11-choline. *J Nucl Med*. 1998;39:990-995.
11. Chen Y, Pullambhatla M, Foss CA, et al. 2-(3-{1-carboxy-5-[(6-[18F]fluoro-pyridine-3-carbonyl)-amino]-pentyl}-ureido)-pen tanedioic acid, [18F]DCFPyL, a PSMA-based PET imaging agent for prostate cancer. *Clin Cancer Res*. 2011;17:7645-7653.
12. Afshar-Oromieh A, Zechmann CM, Malcher A, et al. Comparison of PET imaging with a (68)ga-labelled PSMA ligand and (18)F-choline-based PET/CT for the diagnosis of recurrent prostate cancer. *Eur J Nucl Med Mol Imaging*. 2014;41:11-20.
13. Picchio M, Spinapolice EG, Fallanca F, et al. 11C]choline PET/CT detection of bone metastases in patients with PSA progression after primary treatment for prostate cancer: Comparison with bone scintigraphy. *Eur J Nucl Med Mol Imaging*. 2012;39:13-26.
14. Krishnamurthy GT, Thomas PB, Tubis M, Endow JS, Pritchard JH, Blahd WH. Comparison of 99mTc-polyphosphate and 18F. I. kinetics. *J Nucl Med*. 1974;15:832-836.

15. Evangelista L, Zattoni F, Guttilla A, et al. Choline PET or PET/CT and biochemical relapse of prostate cancer: A systematic review and meta-analysis. *Clin Nucl Med*. 2013;38:305-314.

16. Cimitan M, Bortolus R, Morassut S, et al. 18F]fluorocholine PET/CT imaging for the detection of recurrent prostate cancer at PSA relapse: Experience in 100 consecutive patients. *Eur J Nucl Med Mol Imaging*. 2006;33:1387-1398.

17. Steiner C, Vees H, Zaidi H, et al. Three-phase 18F-fluorocholine PET/CT in the evaluation of prostate cancer recurrence. *Nuklearmedizin*. 2009;48:1-9; quiz N2-3.

18. DeGrado TR, Coleman RE, Wang S, et al. Synthesis and evaluation of 18F-labeled choline as an oncologic tracer for positron emission tomography: Initial findings in prostate cancer. *Cancer Res*. 2001;61:110-117.

19. Chondrogiannis S, Marzola MC, Grassetto G, et al. New acquisition protocol of 18F-choline PET/CT in prostate cancer patients: Review of the literature about methodology and proposal of standardization. *Biomed Res Int*. 2014;2014:215650.

20. ^{11}C-Chlonine. SNMMI PET Center of Excellence and the Center for Molecular Imaging Innovation & Translation. http://snmmi.files.cms-plus.com/ Choline%20chloride%20C-11%20(3).pdf.

21. Bluemel C, Krebs M, Polat B, et al. 68Ga-PSMA-PET/CT in patients with biochemical prostate cancer recurrence and negative 18F-choline-PET/CT. *Clin Nucl Med*. 2016;41:515-521.

22. Szabo Z, Mena E, Rowe SP, et al. Initial evaluation of [(18)F]DCFPyL for prostate-specific membrane antigen (PSMA)-targeted PET imaging of prostate cancer. *Mol Imaging Biol*. 2015;17:565-574.

23. Afshar-Oromieh A, Malcher A, Eder M, et al. PET imaging with a [68Ga]gallium-labelled PSMA ligand for the diagnosis of prostate cancer: Biodistribution in humans and first evaluation of tumour lesions. *Eur J Nucl Med Mol Imaging*. 2013;40:486-495.

24. Herrmann K, Bluemel C, Weineisen M, et al. Biodistribution and radiation dosimetry for a probe targeting prostate-specific membrane antigen for imaging and therapy. *J Nucl Med*. 2015;56:855-861.

25. Afshar-Oromieh A, Hetzheim H, Kratochwil C, et al. The theranostic PSMA ligand PSMA-617 in the diagnosis of prostate cancer by PET/CT: Biodistribution in humans, radiation dosimetry, and first evaluation of tumor lesions. *J Nucl Med*. 2015;56:1697-1705.

26. Afshar-Oromieh A, Hetzheim H, Kubler W, et al. Radiation dosimetry of (68)ga-PSMA-11 (HBED-CC) and preliminary evaluation of optimal imaging timing. *Eur J Nucl Med Mol Imaging*. 2016;43:1611-1620.

27. Afshar-Oromieh A, Sattler LP, Mier W, et al. The clinical impact of additional late PET/CT imaging with 68Ga-PSMA-11 (HBED-CC) in the diagnosis of prostate cancer. *J Nucl Med*. 2017.

28. Rowe SP, Macura KJ, Mena E, et al. PSMA-based [(18)F]DCFPyL PET/CT is superior to conventional imaging for lesion detection in patients with metastatic prostate cancer. *Mol Imaging Biol*. 2016;18:411-419.

9